



LUND UNIVERSITY

ERBB3 is a marker of a ganglioneuroblastoma/ganglioneuroma-like expression profile in neuroblastic tumours

Wilzen, Annica; Krona, Cecilia; Sveinbjornsson, Baldur; Kristiansson, Erik; Dalevi, Daniel; Øra, Ingrid; De Preter, Katleen; Stallings, Raymond L.; Maris, John; Versteeg, Rogier; Nilsson, Staffan; Kogner, Per; Abel, Frida

Published in:
Molecular Cancer

DOI:
[10.1186/1476-4598-12-70](https://doi.org/10.1186/1476-4598-12-70)

2013

[Link to publication](#)

Citation for published version (APA):

Wilzen, A., Krona, C., Sveinbjornsson, B., Kristiansson, E., Dalevi, D., Øra, I., De Preter, K., Stallings, R. L., Maris, J., Versteeg, R., Nilsson, S., Kogner, P., & Abel, F. (2013). ERBB3 is a marker of a ganglioneuroblastoma/ganglioneuroma-like expression profile in neuroblastic tumours. *Molecular Cancer*, 12, Article 70. <https://doi.org/10.1186/1476-4598-12-70>

Total number of authors:
13

General rights

Unless other specific re-use rights are stated the following general rights apply:

Copyright and moral rights for the publications made accessible in the public portal are retained by the authors and/or other copyright owners and it is a condition of accessing publications that users recognise and abide by the legal requirements associated with these rights.

- Users may download and print one copy of any publication from the public portal for the purpose of private study or research.
- You may not further distribute the material or use it for any profit-making activity or commercial gain
- You may freely distribute the URL identifying the publication in the public portal

Read more about Creative commons licenses: <https://creativecommons.org/licenses/>

Take down policy

If you believe that this document breaches copyright please contact us providing details, and we will remove access to the work immediately and investigate your claim.

LUND UNIVERSITY

PO Box 117
221 00 Lund
+46 46-222 00 00

RESEARCH**Open Access**

ERBB3 is a marker of a ganglioneuroblastoma/ganglioneuroma-like expression profile in neuroblastic tumours

Annica Wilzén¹, Cecilia Krons², Baldur Sveinbjörnsson^{2,3}, Erik Kristiansson⁴, Daniel Dalevi⁴, Ingrid Øra⁵, Kathleen De Preter⁶, Raymond L Stallings⁷, John Maris⁸, Rogier Versteeg⁹, Staffan Nilsson⁴, Per Kogner² and Frida Abel^{1*}

Abstract

Background: Neuroblastoma (NB) tumours are commonly divided into three cytogenetic subgroups. However, by unsupervised principal components analysis of gene expression profiles we recently identified four distinct subgroups, r1-r4. In the current study we characterized these different subgroups in more detail, with a specific focus on the fourth divergent tumour subgroup (r4).

Methods: Expression microarray data from four international studies corresponding to 148 neuroblastic tumour cases were subject to division into four expression subgroups using a previously described 6-gene signature. Differentially expressed genes between groups were identified using Significance Analysis of Microarray (SAM). Next, gene expression network modelling was performed to map signalling pathways and cellular processes representing each subgroup. Findings were validated at the protein level by immunohistochemistry and immunoblot analyses.

Results: We identified several significantly up-regulated genes in the r4 subgroup of which the tyrosine kinase receptor *ERBB3* was most prominent (fold change: 132–240). By gene set enrichment analysis (GSEA) the constructed gene network of *ERBB3* (n = 38 network partners) was significantly enriched in the r4 subgroup in all four independent data sets. *ERBB3* was also positively correlated to the ErbB family members *EGFR* and *ERBB2* in all data sets, and a concurrent overexpression was seen in the r4 subgroup. Further studies of histopathology categories using a fifth data set of 110 neuroblastic tumours, showed a striking similarity between the expression profile of r4 to ganglioneuroblastoma (GNB) and ganglioneuroma (GN) tumours. In contrast, the NB histopathological subtype was dominated by mitotic regulating genes, characterizing unfavourable NB subgroups in particular. The high ErbB3 expression in GN tumour types was verified at the protein level, and showed mainly expression in the mature ganglion cells.

Conclusions: Conclusively, this study demonstrates the importance of performing unsupervised clustering and subtype discovery of data sets prior to analyses to avoid a mixture of tumour subtypes, which may otherwise give distorted results and lead to incorrect conclusions. The current study identifies *ERBB3* as a clear-cut marker of a GNB/GN-like expression profile, and we suggest a 7-gene expression signature (including *ERBB3*) as a complement to histopathology analysis of neuroblastic tumours. Further studies of ErbB3 and other ErbB family members and their role in neuroblastic differentiation and pathogenesis are warranted.

Keywords: Microarray, Expression, Cancer, Systems biology, Oncology, Network, Reverse engineering, Unsupervised, Clustering, Cell cycle, Spindle assembly, Her-3, HER3, ERBB3, Her-2, HER2, ERBB2, EGFR, ERBB1, BIRC5, Survivin, MYCN, N-myc, ALK, PHOX2B, NTRK1, CCND1

* Correspondence: frida.abel@gu.se

¹Department of Clinical Genetics, Institution of Biomedicine, Box 413, S- 405 30, Gothenburg University, Gothenburg, Sweden

Full list of author information is available at the end of the article

Background

Peripheral neuroblastic tumours (NT's) are derived from developing neuronal cells of the sympathetic nervous system and are the most frequent extracranial solid tumours of childhood. NT's are composed of variable proportion of neuroblasts (neuronal lineage) and Schwannian cells (glial lineage), and are classified into histopathological categories according to the presence or absence of Schwannian stromal development, differentiation grade of the neuroblasts, and their cellular turnover index. According to the International Neuroblastoma Pathology Classification (INPC - Shimada system) [1], the three subtype categories and their subtypes are: 1) Neuroblastoma (NB), Schwannian stroma-poor; 2) ganglioneuroblastoma (GNB), intermixed (Schwannian stroma-rich) or nodular (composite Schwannian stroma-rich/stroma-dominant and stroma-poor); 3) ganglioneuroma (GN), Schwannian stroma-dominant. Neuroblastoma exhibit an extreme clinical and biological heterogeneity, and patients are assigned to risk groups based on several criteria including stage [2,3], age [4], histological category and grade of tumour differentiation (histopathology) [5], the status of the *MYCN* oncogene [6], chromosome 11q status [7], and DNA ploidy [8] as the most highly statistically significant and clinically relevant factors [9]. One-half of NB patients have metastatic disease at diagnosis (INSS stage 4 or INRGSS stage M). All metastatic tumours with *MYCN* amplification (MNA) are aggressive and considered being high-risk tumours [9], whereas children with metastatic disease without MNA (approximately 65%) have variable clinical behaviours depending on age at diagnosis, histopathology, and other genetic factors. Based upon cytogenetic profiles, previous studies have categorized NB tumours into three major subtypes [10,11]: Subtype 1 representing favourable tumours with near triploidy and high expression of the Neurotrophic receptor TrkA (or NTRK1), mostly encompassing non-metastatic NB stages 1 and 2; subtype 2A representing unfavourable NB stages 3 and 4, with 11q deletion (Del11q) and 17q gain (Gain17q) but without MNA; subtype 2B representing unfavourable widespread NB stages 3 and 4 with MNA often together with 1p deletion (Del1p) and Gain17q. Several gene sets are shown to discriminate the molecular subgroups and risk groups by mRNA and microRNA expression profiling in neuroblastic tumours [12-21]. A recent expression analysis by our research group identified the three cytogenetically defined subtypes (1, 2A, and 2B) by unsupervised clustering, but further indicated the existence of a fourth divergent subgroup [12]. Moreover, we identified a 6-gene signature including *ALK*, *BIRC5*, *CCND1*, *MYCN*, *NTRK1*, and *PHOX2B* to successfully discriminate these four subgroups [12]. The fourth (r4) subgroup encompassed tumours characterized by Del11q and high expression of genes involved in the

development of the nervous system, but showed low expression of *ALK*. Approximately 7-9% of sporadic NB cases show inherent *ALK* mutations [22,23], and *ALK* overexpression, both in its mutated and wild type form, is demonstrated to define a poor prognosis in NB patients [24]. In relation to this our previous findings suggests the Type 2A (r2) and Type 2B (r3) subgroups, which both display high *ALK* expression, to be driven by the *ALK* pathway. In contrast, the r4 subgroup displaying low expression of all six genes of the signature, is suggested to be driven by an alternative oncogenesis pathway.

In the present study we aimed to further investigate the expression profiles of the four subgroups, and r4 in particular. By differential expression analysis and reverse engineering we found *ERBB3* and its network members to be significantly overrepresented within the r4 tumour subgroup. Moreover, two other ErbB family members, *ERBB2* and *EGFR*, were found to show concurrently higher expression. In contrast, unfavourable neuroblastoma subgroups (r2 and r3) were specifically characterized by G2/M cell cycle transition and mitotic regulating genes. By expression analysis of histopathology categories (i.e. NBs, GNBs, and GNs) we found the r4 subgroup to show an identical expression profile to GNB/GN types, and overexpression of ErbB3 was also confirmed at the protein level in GN tumours. We conclude that the ERBB-profile (high expression of *EGFR*, *ERBB2* and *ERBB3*) defines a ganglion-rich neuroblastic tumour sub-set.

Results

Differential expression in r-subgroups

To explore subgroup-specific characteristics we performed a differential expression analysis by SAM. Thirty-seven tumour cases from three studies were pre-processed in two separate data sets (data set 1, n = 14, and data set 2, n = 23, Table 1), and both data sets were divided into four r-subgroups based on rules according to the previously described 6-gene signature (6-GeneSig, Additional file 1) [12]. Six SAM pair-wise comparisons between r-subgroups were performed on each data set separately, and the 1000 most significant genes (according to descending SAM d-score) with a fold change above 2, were extracted to create SAM_{intersect} gene lists representing both data sets (Additional file 2). The r2 versus r1 group comparison showed 122 differentially expressed genes present in lists from both data sets, and the r3 versus r1 group comparison showed 496 overlapping genes (Figure 1A). The r4 subgroup showed the highest proportion of significant differentially expressed genes compared to all the other subgroups in both data sets (number of overlapping genes ranging between 503 and 669, Figure 1A).

Table 1 Data sets used in the current study

	Name	Reference	# Total cases	Description	Analysis platform	# Analysis cases	Analysis groups	Purpose of study
Data set 1	DePreter	[53]	17	Neuroblastoma	Affy HU133A (pre-amplified)	14	r-groups (r1-r4)	Differential mRNA expression of subgroups
Data set 2	McArdle	[54]	22	Neuroblastic	Affy HU133A	17	r-groups (r1-r4)	Differential mRNA expression of subgroups
	Wilzén	[55]	8	Neuroblastoma	Affy HU133A	6	r-groups (r1-r4)	Differential mRNA expression of subgroups
Data set 3	Wang	[56]	101	Neuroblastoma	Affy HGU95Av	67	r-groups (r1-r4)	Verification of subgroup findings; Gene network construction
Data set 4	Versteeg	[57]	110	Neuroblastic	Affy HU133plus2	110	Histology groups (GN, GNB, NB)	Differential mRNA expression of histology subgroups
Data set 5	Kogner	-	12*	Neuroblastic	IHC, WB	8 (IHC), 9 (WB)	Histology groups (GN, NB)	Protein expression validation in histology subgroups

SAM Significance Analysis of Microarray. Neuroblastic = mixed pool of neuroblastoma (NB), ganglioneuroblastoma (GNB), and ganglioneuroma (GN). Affy Affymetrix, IHC Immunohistochemistry, WB Western blotting.* One case overlaps with data set 2 (case "NBS1" in data set 2 = case '6' in data set 5).

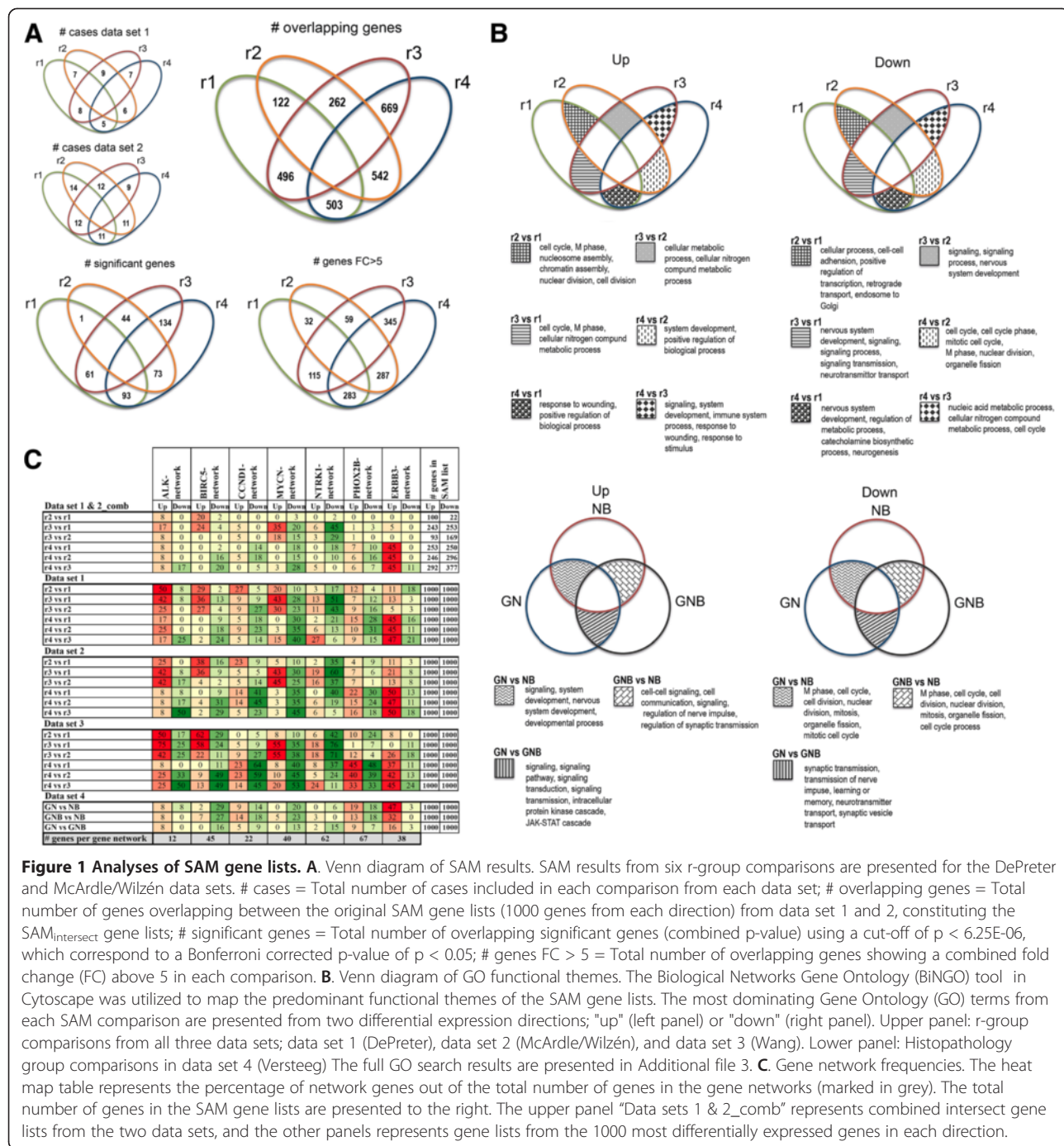
The r1 subgroup (corresponding to the cytogenetically defined subgroup Type 1) was found to mainly involve nervous system developmental and catecholamine metabolic process related genes. In the MNA-specific subgroup r3 (corresponding to Type 2B), *KIF15* was the most significantly up-regulated gene (fold = 15) while *CUX2* showed the highest expression fold change (fold = 17). The *MYCN* gene was found on the 74th position of up-regulated genes (fold = 9), and *NTRK1* was identified as the most significantly down-regulated gene within r3 compared to r1 (fold = 80, Additional file 2). Also, *LMO3* and *PHGDH* were found to be specifically up-regulated in the r3 subgroup compared to the other subgroups. High expression of *ALK* was found in both the r2 (2-fold) and r3 (5-fold) subgroups compared to the favourable r1 subgroup. Moreover, r2 and r3 also showed up-regulation of several G2/M cell cycle transition and mitotic checkpoint related genes (e.g. *AURKA*, *BRCA1*, *BUB1B*, *CCNA2*, *CCNB1*, *KIF15*, *MCM2*, *MCM3*, and *MCM5* etc.), which in contrast showed a significant down-regulation in the r4 subgroup. In line with this, a Gene Ontology (GO) search identified "cell cycle" as the most significant process accumulated in the SAM_{intersect} gene lists of the r2 and r3 subgroups (Figure 1B, Additional file 3). The apparent overrepresentation of cell cycle-related genes in subgroups r2 and r3 encouraged us to investigate enrichment of other cell cycle key players and networks in our SAM gene lists.

Differential expression in subgroup r4

Among the 10 most significantly up-regulated genes in the r4 subgroup in data sets 1 and 2, the following eleven genes were found; *ABCA8*, *APOD*, *ASPA*, *CDH19*, *ERBB3*, *FXYD1*, *ITIH5*, *MAL*, *PLP1*, *S100B*, and *ST6GALNAC2*. According to the GO search, these genes are mainly involved in nervous system development, multicellular organismal

development, and response to wounding (Figure 1B, Additional file 3). *ERBB3* was found as the "top-one" up-regulated gene in r4 versus r3 with a 240-fold expression. *ERBB3* encodes a transmembrane tyrosine kinase receptor, which has previously been associated with cancer in a large number of studies (>500 publications). ErbB3 is activated through dimerization to one of its four structurally related family members; EGFR, ErbB2, or ErbB4. ErbB-family members are often co-expressed, and thus we found it relevant to investigate their expression level relationships in our four neuroblastic data sets. We found a positive significant correlation of *ERBB3* to the *EGFR* and *ERBB2* family members, and a negative correlation to all genes of the 6-GeneSig in all four data sets ($p < 0.05$, Additional file 4). Also, *EGFR* and *ERBB2* showed a significant up-regulation in r4 subgroups of most data sets ($p < 0.05$, Additional file 2). *ERBB3* show several similarities to *ALK*, encoding the NB familial gene [25], and thus made a good candidate gene with potential role in the tumour development of r4 tumour types.

Among the down-regulated genes in the r4 subgroup *CACNA2D3* was the most significant in comparison to the r1 subgroup (50-fold change). This gene was also found to be the 25th most down-regulated gene in the r3 subgroup compared to r1 (Additional file 2). Since both the r3 and r4 subgroups are previously found to show unfavourable outcome and poor survival [12], and the *CACNA2D3* gene is located in the 3p21.1- locus commonly deleted in many NB tumours, this encouraged us to further screen the SAM_{intersect} gene lists for other conceivable and previously reported tumour suppressor (TS) candidate genes. Out of 33 previously reported TS candidate genes, 15 were present among the SAM_{intersect} gene lists from data sets 1 and 2 (Additional file 5).



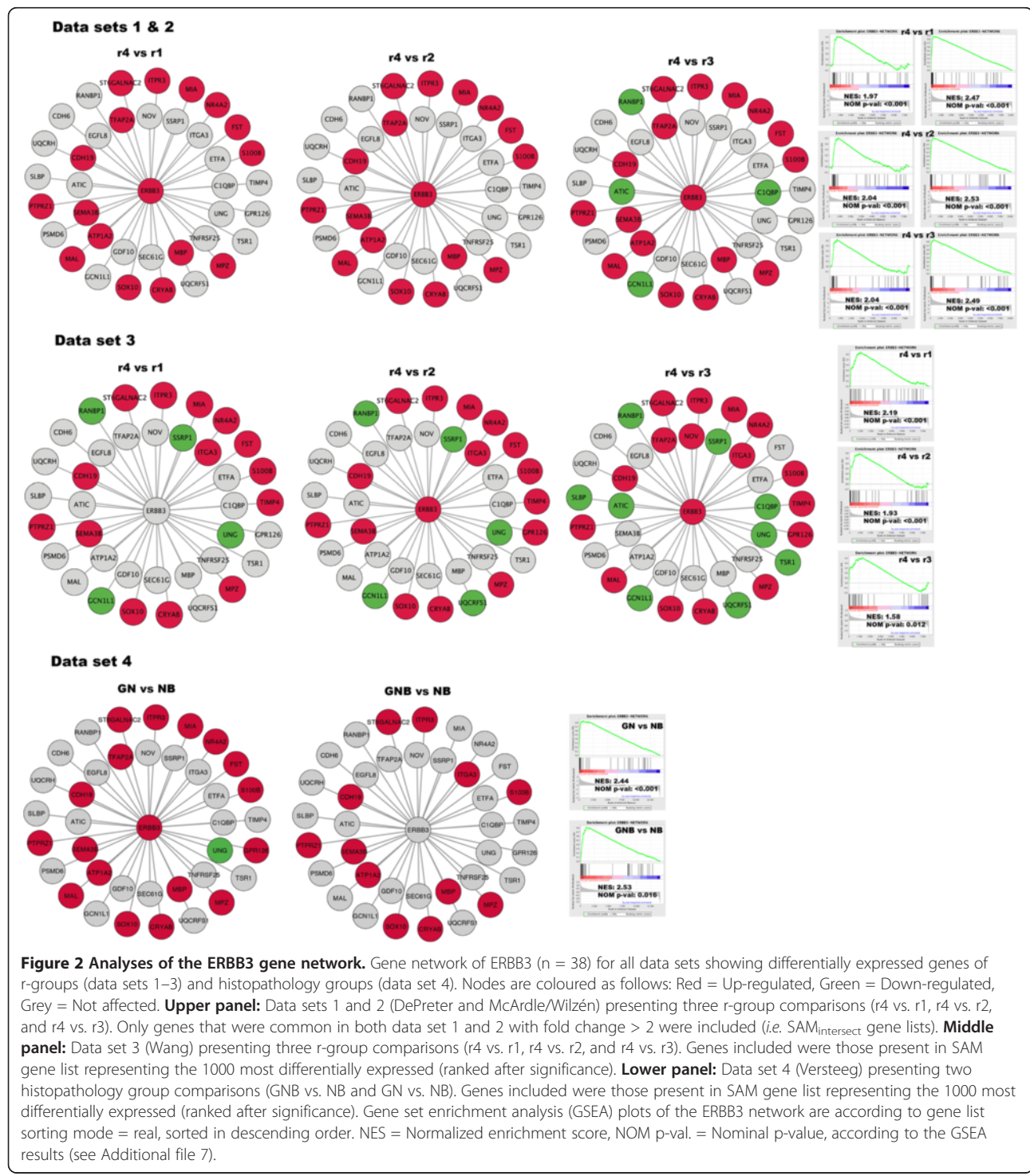
Gene network construction and gene set enrichment analysis (GSEA)

Network modelling reveals the regulatory relationships among genes and can provide a systematic understanding of molecular mechanisms underlying biological processes. A variety of algorithms have been developed, and in the current study we chose the ARACNE algorithm [26] for reconstruction of seven networks (*ALK*, *BIRC5*, *CCND1*, *ERBB3*, *MYCN*, *NTRK1*, *PHOX2B*) from the Wang data set

($n = 102$), since this method has a documented high performance [27]. Also, 4850 pre-existing curate gene sets (c2) from the Molecular Signatures Database (MSigDB) were selected (Additional file 6). We subsequently analysed the lists of differentially expressed genes for enrichment of these 4850 gene networks. The SAM_{intersect} lists of genes up-regulated in the r4 group were found to comprise 17 out of 38 partners (~ 45%) of the ARACNE_ERBB3 network (Figure 1C), which was significantly verified by GSEA ($p < 0.001$,

Figure 2, Additional file 7). A relatively large fraction (between 20% and 58%) of the ARACNE_BIRC5 network partners ($n = 45$, Additional file 6) were found among the up-regulated genes of r2 and r3 tumour subgroups, which was also significant by GSEA ($p < 0.001$, Additional file 7). A GO search of the BIRC5 network partners suggested a role

in mitosis (GO terms: cell cycle, nucleosome assembly, chromatin assembly, protein-DNA complex assembly, nucleosome organization, mitotic cell cycle, cell cycle phase, DNA packaging, M phase, and cell cycle process, data not shown). Other cell-cycle or mitotic related gene sets found to be enriched among the r2 and r3 subgroups were e.g.



ZHOU_CELL_CYCLE_GENES_IN_IR_RESPONSE_24HR, WHITFIELD_CELL_CYCLE_LITERATURE, REACTOME_CELL_CYCLE_MITOTIC, REACTOME_CELL_CYCLE_CHECKPOINTS curate gene sets (Additional file 7).

Verification of gene network modelling and differential expression analysis

The differential expression profiles of the r-subgroups were verified by replicating the study using the Wang data set ($n = 67$ cases, Table 1). The outcomes of SAM were in consistence with previous findings, showing the *ERBB3* gene to be significantly up-regulated and its gene-network partners to be significantly overrepresented in the r4 subgroup (Figure 1C, Figure 2). Also, several other previously identified r4-specific genes, *APOD*, *CDH19*, *FXYD1*, and *S100B*, were found among the 1000 most significantly up-regulated genes. In concordance with the previous analysis, we found the expression of *CUX2* (fold = 5), *LMO3* (fold = 2.7) and *PHGDH* (fold = 1.9) to be significantly higher in the MNA subgroup (r3) compared to the favourable subset (r1). In addition, cell cycle-related genes dominated the r2 and r3 subgroups, and this was significantly proven by GSEA of the BIRC5 network and other cell cycle networks ($p < 0.001$, Additional file 7).

To confirm the robustness of the ARACNE constructed gene networks, we selected the r3 versus r1 comparisons in data sets 1 and 2 to investigate the expected overrepresentation of MYCN- and NTRK1-network partners. Fourteen genes out of 40 (35%) of the ARACNE_MYCN network were found in the up-regulated gene lists, while eight out of 40 (20%) genes were found in the down-regulated gene lists, demonstrating an accumulation of the ARACNE_MYCN network in the r3 subgroup (Figure 1C, Additional files 7 and 8). Also, an accumulation of the ARACNE_NTRK1 network was found in the opposite direction. Out of 62 genes composing the ARACNE_NTRK1 network, 28 genes (~45%) were among the 1000 most down-regulated genes in r3, which was significant by GSEA (Additional files 7 and 8). According to significance by SAM, the *NTRK1* gene was the “top-one” down-regulated gene within the r3 versus r1 subgroup comparison in both data sets (fold change: >70, Figure 1C, Additional file 2). From these facts we conclude our study design to be substantial, and the constructed gene networks by ARACNE to be reliable and highly representative.

In addition, we checked the enrichment of network partners to the 6-GeneSig (*ALK*, *BIRC5*, *CCND1*, *MYCN*, *NTRK1*, and *PHOX2B*) and found the network representations to be in concordance with the 6-GeneSig expression levels in r-subgroups (Additional file 7). The credibility of ARACNE constructed networks were also tested by literature verification, and seven out of 38 transcriptional connections of the ERBB3-network as well as 11 out of 40

transcriptional connections of the MYCN-network were verified to have a functional relationship (data not shown). This demonstrates the robustness of the computationally inferred network analysis.

Differential expression analysis of histopathology groups (data set 4)

To further explore the *ERBB3* expression among other neuroblastic tumour we utilized the R2 database (hgserver1.amc.nl), and found indications of high *ERBB3* expression in GNB and GN tumours. To investigate this finding in more detail, we performed a differential expression analysis of the histopathology subtypes in the Versteeg 110 data set ($n = 110$, Table 1). As expected, the *ERBB3* gene and networks partners were significantly enriched in GNB and GN tumours compared to NB (Figure 1C, Additional file 7). The highest enrichment of the ERBB3-network was found in GN tumours, with 18 up-regulated genes out of 38 ($p < 0.001$, Figure 2). In contrast, cell cycle-related genes and gene networks significantly dominated the NB types, including the ARACNE_BIRC5 network (Additional files 2 and 7).

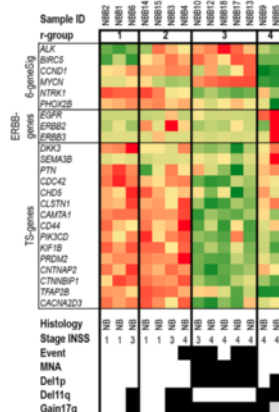
Subgroup-specific expression profiles

ErbB family member genes (*ERBB*-genes; *EGFR*, *ERBB2*, and *ERBB3*) and 15 previously reported tumour suppressor candidate genes (TS-genes) were next studied by heat maps in all four data sets (Figure 3). Most TS candidate genes were down-regulated in the MNA-specific r3 subgroup only. However, the *CTNNB1P1* and *KIF1B* transcripts were also found to be down-regulated in both r3 and r4 subgroups, and the *TFAP2B* transcript was specifically down-regulated in the r4 subgroup alone (Figure 3, Additional file 2). Overall, the expression profiles of the 6-GeneSig genes, *ERBB*-genes, and TS-genes (25 genes in total) among r-subgroups were very similar between data sets. Moreover, the expression profiles of the GNB/GN tumours were identical to the previously detected r4 subgroups of NB (Figure 3). These results strongly indicate that the same cellular pathways are active in r4 and GNB/GN tumours types, hence the ERBB-gene profile most likely represents a more differentiated subset of tumours.

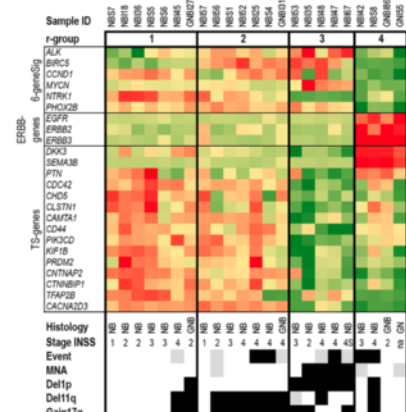
Verification of ErbB3 at protein level (data set 5)

To validate the biological significance of the *ERBB3* enrichment in the expression profiles of GN tumours, the ErbB3 protein expression was investigated by immunohistochemistry (IHC) and western blot (WB) analysis. The IHC was performed on formalin-fixed and paraffin-embedded (FFPE) tissue slides from four GN and four NB tumours by using antibodies specific for Sox10 ([N-20], Santa Cruz Biotechnology) and ErbB-3 ([RTJ2], Abcam) respectively. The IHC showed ErbB3 to be mainly expressed in mature ganglion cells, whereas Sox10 was expressed in both ganglion and

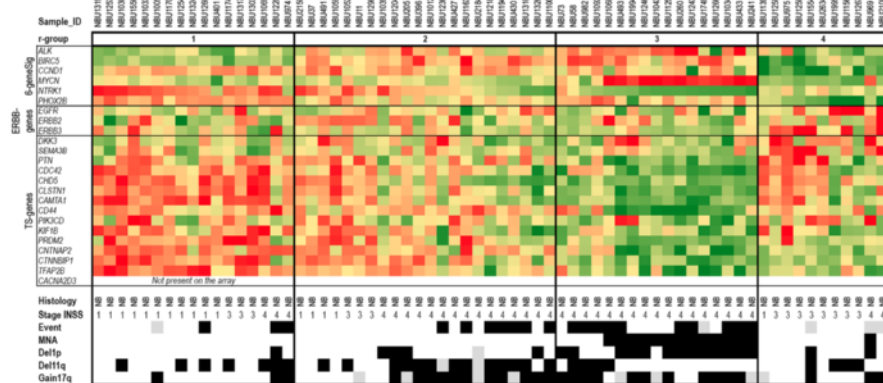
Data set 1: De Preter



Data set 2: McArdle-Wilzén



Data set 3: Wang



Data set 4: Molenaar

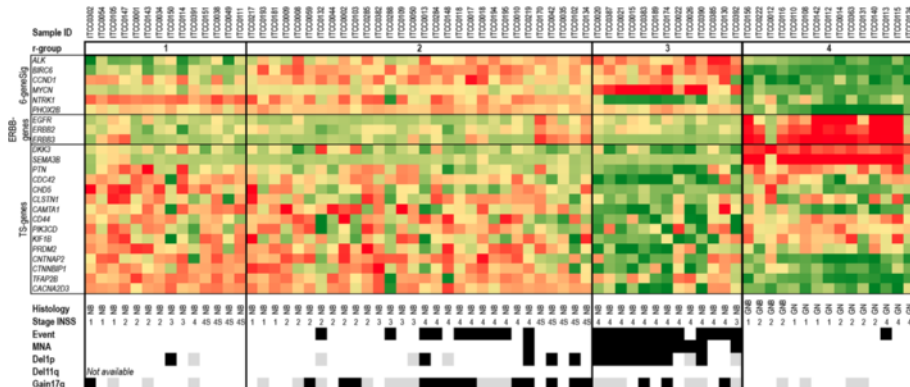


Figure 3 Heat maps of r-subgroups. Heat map of the 6-GeneSig (*ALK*, *BIRC5*, *CCND1*, *MYCN*, *NTRK1*, and *PHOX2B*), ERBB-genes (*EGFR*, *ERBB2*, and *ERBB3*) and 15 TS-genes (Tumour suppressor candidate genes) for all four data sets. The heat map colour scale is based on standard deviations (sd) of all cases in each data set separately, and ranges from sd = 2 (red) to sd = -2 (green). The lower panel represents clinical and biological markers: Histopathology, NB = Neuroblastoma, GNB = ganglioneuroblastoma, GN = ganglioneuroma; Stage INSS, clinical stages 1–4, and 4S according to the international staging system, na = not available; Event = dead of disease, MNA = *MYCN* amplification, Del1p = 1p deletion, Del11q = 11q deletion, Gain17q = gain of 17q. Colour coding: white = no event, black = event, grey = not available.

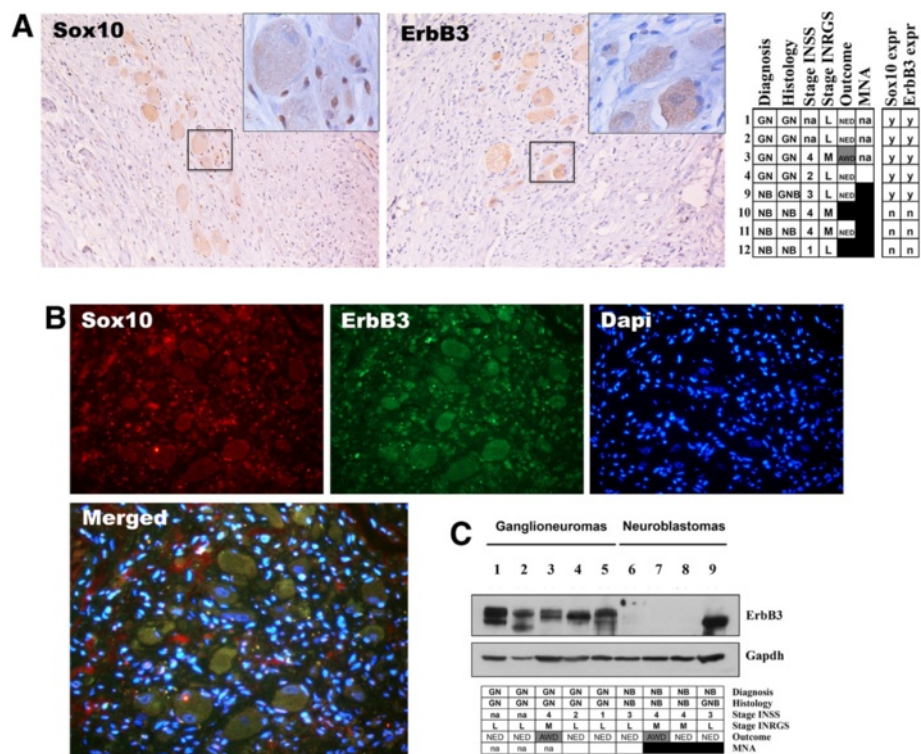


Figure 4 Protein expression validation of ErbB3. A. Immunohistochemistry (IHC) assessment of case 2 showing ErbB3 expression in the mature ganglion cells, and Sox10 expression in both ganglion and schwannian cells. Tumour tissue sections were stained using horseradish peroxidase (HRP) secondary antibodies. The right panel shows the Sox10 and ErbB3 expression results from all IHC assessments performed, y = yes, n = no expression. **B.** Colocalization study of ErbB3 and Sox10, showing ErbB3 expression mainly in ganglion cells. Tumour tissue sections were simultaneously fluorescently stained using anti-goat Alexa Fluor 594 (Sox10, red) and anti-mouse Alexa Fluor 488 (ErbB3, green), and Dapi (DNA, blue). **C.** High protein levels in GN tumours shown by Western blot of ErbB3. Primary antibodies used in studies: Sox10 ([N-20], Santa Cruz Biotechnology), and ErbB3-3 ([RTJ2], Abcam), which binds to both phosphorylated and unphosphorylated forms. Case 6 was also included in the microarray analysis (NBS1, data set 2). Clinical data: NB = neuroblastoma, GNB = ganglioneuroblastoma, GN = ganglioneuroma; INSS stage [2]; INRGs stage [3]: L = Localised, L1/L2 (INSS 1, 2, 3); M = Metastatic (INSS 4); Outcome: NED = No evidence of disease (white); AWD = Alive with disease (grey); DOD = Dead of disease (black); MNA (MYCN-amplification), black = yes, white = no, na = not applicable.

schwannian cells (Figure 4A-B). A high fraction of satellite cells, as well as schwannian cells were also Sox10 immunopositive (data not shown).

Immunoblot analysis was performed on five GN and four NB in total (data set 5, Table 1). Out of the five investigated GN cases, four corresponded to the GN cases examined by IHC. In addition, the WB analysis also included one NB encompassed in the microarray analysis (case 6 corresponding to NBS1 in data set 2). The same antibody as for IHC ([RTJ2], Abcam) directed against the cytoplasmic region of ErbB3 was chosen in order to detect several isoforms of the protein as well as post-translationally modified and unmodified forms. Overall, ErbB3 expression levels were high and clearly enriched in the GN subset compared to the NB subset, which showed no detectable levels of ErbB3. Moreover, case 6/NBS1 previously displaying no or very low expression of *ERBB3* by microarray analysis (data set 2, Figure 3), showed no detectable levels of ErbB3 at protein level by immunoblot analysis. Only one of the NB tumours (case 9) showed a strong

ErbB3 signal. However, this case was a localized INSS stage 3 with favourable biology, later histopathologically classified as a GNB. Moreover, only the lower molecular weight band was visible indicating that the protein might be in its inactive unphosphorylated form, or indicate other post-translational modification or isoforms of ErbB3 (Figure 4C).

Histopathology classification

Based on our results we included *ERBB3* in the 6-GeneSig thus creating a new 7-GeneSig. The 7-GeneSig was refined to discriminate five subclasses; “NB-r1”, “NB-r2”, “NB-r3”, “GNB-r4”, and “GN-r4” (Additional file 9). In order to test the robustness of this 7-GeneSig subgroup classification, cases from all data sets were reclassified into three histopathology prediction classes “NB” (NB-r1, NB-r2, NB-r3), “GNB” (GNB-r4), and “GN” (GN-r4) and the reliability of assignments were investigated. Out of 110 neuroblastic tumours of the Versteeg data set, 82 cases could be successfully assigned according to the 7-GeneSig rules (Additional

file 9). All NB histopathology types (64 out of 64) were correctly assigned according to the 7-GeneSig, and the inter-rate reliability of assignments was highly significant (Kappa measure of agreement $p = 7.489E-17$, Table 2). Five out of eight GNB tumour types, as well as nine out of ten GN tumour types were correctly assigned. One GN was predicted as "GNB" according to the 7-GeneSig (Table 2). In addition, we also performed a reassignment test on data set 2 comprising one GN, four GNB, and 25 NB tumour types, which was also significant (inter-rate reliability $p = 0.003$, data not shown). Reassignment of r4-cases (from data sets 1, 2 and 3), previously classified as NB, were all assigned to the "GNB" or "GN" categories by the 7-GeneSig. Also, all NB cases of data set 4 fell into the NB r1-r3 categories (data not shown). Conclusively, the histopathology classification and subgroup assignment by the 7-GeneSig seemed reliable and highly predictive.

Discussion

Neuroblastic tumours (NT's) represent a spectrum of disease, from undifferentiated and aggressive NB to the differentiated and largely quiescent GN tumours. NB tumours are commonly categorized into three main types based on numerical and structural genomic alterations, as well as expression of the neurotrophin receptor TrkA [10]. In a recent study using Principal Components Analysis (PCA) however, our data indicated the existence of four molecular tumour groups, r1-r4 [12]. In the current study we aimed to further characterize these four molecular subgroups, and investigated the divergent r4 group in particular. While the r2 (Type 2A) and r3 (Type 2B) tumour subgroups were dominated by cell cycle-related genes and networks, those were completely absent in the r4 subgroups (data sets 1-3) and GNB or GN subtypes (data set 4). The vast majority of the cell cycle-related genes were linked to the G2/M transition and spindle assembly checkpoint (e.g. *BIRC5*, *BRCA1*, *BUB1B*, *CCNA2*, *CCNB1*, *FANCI*, *HMMR*, *KIF15*, and

MCM2), many of which were found to belong to the ARACNE-modelled BIRC5-network. Overexpression of genes involved in mitotic regulation is typical for rapidly proliferating tumours and would also be expected to be enriched in the aggressive NB subtypes when compared to more differentiated quiescent GNB and GN tumours. The BIRC5 protein is found to stabilize the microtubules in the chromosomal passenger complex, and knockdown of *BIRC5* causes apoptosis in NB via mitotic catastrophe [28]. Also, a previous publication show that NB tumours with genomic aberrations in G1-regulating genes leads to S and G2/M phase progression [20]. Interestingly, the fork head box (FOX) gene *FOXM1* encoding a protein phosphorylated in M phase was significantly up-regulated in r2 and r3 subgroups. *FOXM1* activates the expression of several cell cycle genes, e.g. *AURKB*, *CCNB1*, *CCND1*, *MYC*, and is involved in cell proliferation and malignancy [29]. Several cell cycle and DNA repair genes, including *BIRC5*, are suggested to act downstream of N-myc [21,30,31]. In addition, most of the studied tumour suppressor (TS) candidates were specifically down-regulated in the r3 subgroup, which is probably explained by them acting downstream of N-myc. Several of the TS candidate genes are also located in the 1p36 chromosomal region (e.g. *CHDS* and *KIF1B* [32-34]), and Del1p is a well-known prognostic marker highly correlated to *MYCN*-amplification in NB [35]. One such N-myc-regulated and 1p36-localized TS candidate is *CDC42*, encoding a small GTPase protein. This protein have a function in cell polarization and growth cone development in NB cell differentiation, similar to Rac1 and Cux-2, and is suggested to inhibit neuritogenesis in NB [36]. In concordance to this, we found *CDC42* to be the 14th most significantly down-regulated gene in the MNA subgroup (r3) compared to subgroup r2.

The main focus of the study was to define the underlying regulatory networks of the r4 subgroup. In contrast to the other three well-known subgroups of NB, the r4 tumours showed high expression of embryonic development and nervous system signalling genes. One of the most prominent genes from the differential expression analysis was *ERBB3*, encoding a member of the epidermal growth factor receptor (EGFR) family of receptor tyrosine kinases (RTK's). The ARACNE-modelled *ERBB3*-network was significantly enriched in the differentially expressed gene lists of the r4 subgroups (data sets 1-3), and this enrichment was also found in the GNB and GN histopathology categories of data set 4. Two members of the *ERBB3*-network, *S100B* and *SOX10*, were among the ten most significantly up-regulated genes in the r4 subgroups. The S100 calcium binding protein B (S100B) has long been reported as a prognostic biomarker of malignant melanoma [37], and a paired down-regulation of *ERBB3* and *S100B* is observed in malignant peripheral nerve sheath tumours confirming their functional relationship [38]. Interestingly, the S100 beta

Table 2 Histology prediction by 7-GeneSig

		Histology			
		NB	GNB	GN	Total:
Predicted	NB	64	0	0	64
	GN	0	1	9	10
	GNB	2	5	1	8
Total:		66	6	10	82
		<i>nd=28</i>			

Measure of agreement (Kappa) $p = 7.489E-17$

Histology prediction was performed on the Versteeg data set ($n = 110$). Group prediction was based upon the standard deviation (sd) of expression of *ALK*, *BIRC5*, *CCND1*, *MYCN*, *NTRK1*, *PHOX2B*, and *ERBB3* according to the rules in Additional file 9. Out of 110 tumours, 82 were successfully assigned and for 28 tumour cases no group belonging could be determined. The groups were assigned as follows: "NB" (r1-r3), "GNB" (r4-GNB), and "GN" (r4-GN). The inter-rate reliability (Kappa) was used to measure the agreement between the assignments of categories ($p = 7.489E-17$).

protein, mapping to chromosome 21, has been proposed to be responsible for the lack of NB in Down syndrome patients by producing growth inhibition and differentiation of neural cells [39]. The SRY box 10 transcription factor (Sox10) is a key regulator of the developing nervous system, and has been shown to control expression of ErbB3 in neural crest cells [40,41]. A paired overexpression of ErbB3 and Sox10 has been observed in pilocytic astrocytoma (PA) a common glioma of childhood, which verifies their network connection found in the current study [42]. Also, Sox10 and S100 are routinely employed in the pathological diagnosis of neural crest-derived tumours [43], and Sox10 serves as an embryonic glial-lineage marker in NT's [44]. By immunohistochemistry assessment, we found Sox10 to be expressed in both the schwannian cells and ganglion cells, whereas ErbB3 was found mainly in the mature ganglion cells. We could also verify the GN-specific expression of ErbB3 by immunoblot analysis.

ErbB3 is activated through ligand binding of neuregulin (NRG), leading to heterodimerization of ErbB3 to other ErbB members and subsequent phosphorylation. Activated ErbB3 regulates proliferation through downstream signalling of the phosphoinositol 3-kinase/AKT survival/mitogenic pathways [25]. In the current study we found a significant correlation of *ERBB3* to its family members *EGFR* and *ERBB2* in all four independent data sets. *EGFR* and *ERBB2* were also both found to be significantly up-regulated in all r4 subgroups as well as in the GNB and GN tumours. Amplification of *ERBB3* and/or overexpression of its protein has been reported in numerous cancers, including prostate, bladder, and breast. Moreover, loss of ErbB3 function has been shown to eliminate the transforming capability of ErbB2 (also known as HER-2) in breast tumours [45]. Although the extent of the role of ErbB3 is emerging, its clinical relevance in different tumours is controversial. There are a few studies of ErbB/HER receptor expression in neuroblastoma, showing that ErbB/HER family members in neuroblastic tumour biology is interrelated and complex, but their expression level may present a prognostic factor for patients outcome [46-48].

The heat map of 25 genes including the 6-GeneSig genes, *ERBB*-genes and TS-genes showed a very specific expression pattern among the different r-subgroups and histopathology categories. The similarity of expression profiles between the four data sets was striking. The correspondence of the r4 subgroups to the GNB and GN histopathology subtypes was obvious, and *ERBB3* appeared as a clear-cut marker for a GNB/GN-like expression profile. To demonstrate this further, a new 7-GeneSig (including *ERBB3*) was constructed and used in a histopathology re-assignment classification test. The 7-GeneSig successfully assigned 100% NB tumours, 62,5% GNB tumours, and 90% GN tumours into the correct histopathology category (Kappa measure of agreement $p = 7.489E-17$, data set 4).

Also, all r4-tumour types from data sets 1–3 were categorized as GNB or GN tumours according to the 7-GeneSig. By these facts we conclude that the NB tumours previously assigned to the r4 subgroup by the 6-GeneSig, most likely represent more differentiated NT's and are seemingly GNB/GN tumours types. Our study brings out the complexity in classifying neuroblastic tumours. The previously described unfavourable characteristics and poor outcome of the r4 tumour group is puzzling [12], but can be explained by the fact that prognostic subsets of GNB's exist [49]. Historically, GNB's have been the most difficult of the NT's to define in a consistent and uniform fashion, because the number and degree of differentiation of the neuroblastic cells tend to vary between cases as well as between different microscopic fields in the same tumour [1]. Moreover, the data sets used in the current study are probably not truly population-based, and the r4 subgroups found probably consist of different proportions of F/UF subsets. In addition, some tumours may previously have been misclassified as NB, or the tumour tissue part analysed by microarray may not be the same as the tissue part that underwent histopathology assessment. Furthermore, it is not clear whether differentiation markers are superior to other prognostic factors in defining outcome. Unfavourable markers such as MNA and clinical stage may also be present in or among differentiated cells, and mark a poor prognosis by themselves.

ErbB3 also has an important role in differentiation of Neural crest cell (NCC) lineages during the embryonic development [50]. Although ErbB receptors are also found to mediate proliferation and survival [47,48], the ERBB-profile found in this study is likely to reflect the phenotype or differentiation stage of developing neuronal progenitors. Upon induction of differentiation, neuronal progenitors may follow a variety of stages of NCC lineages. For example, neuroblasts in culture are shown to represent an immature bilineage stage able to progress towards neuronal and glial fates [44]. Schwannian cells are the principal glia of the peripheral nervous system, whereas neuroblasts differentiate from neural stem cells and exhibit variable degrees of differentiation up to ganglion cells. In this context, the ERBB-profile seems to be a marker of ganglionic-neuronal differentiation. A recent immunohistochemistry study of ErbB2 in neuroblastic tumours supports this conclusion [51]. However, it still remains uncertain whether the r4 subgroup of datasets 1 and 3 are indeed GN or GNB, or if the ERBB expression profile just marks the gradually differentiated NB tumours (encompassing increased levels of mature ganglion cells). Nevertheless, the results from all data sets are consistent in regards to the expression profile of the 25 genes selected for the heat map, strengthening the robustness of the suggested 7-gene signature. Accordingly, we propose ErbB3 as an excellent marker of neuronal differentiation, and suggest mRNA expression profiling by the 7-gene signature as a complement to

histopathological assessment. However, the exact cut-off expression levels for classification needs to be worked out in more detail, and classification must be based on international standard cases and assays.

Conclusions

In summary, by differential expression analysis and network modelling we have identified genes and gene networks constituting molecular and histological subgroups of neuroblastic tumours. The primary aim of our study was to identify genes characterizing the previously unknown r4 subgroup. Our results pinpointed *ERBB3* and its network as one of the most significantly up-regulated genes within this group. By studying the expression profiles in a broader range of neuroblastic tumour types, we found the r4 subgroup to be highly similar to GNB/GN tumour types. The ERBB-dominated profile found in r4 and GNB/GN tumours was clearly divergent from the cell-cycle-dominating profile mainly representing NB tumour subgroups (specifically unfavourable NB subgroups). Our findings indicate that the previously identified r4 subgroup most likely constitutes GNB/GN tumours or NB tumours with high content of mature ganglion cells. This study also demonstrates the importance of performing unsupervised subtype clustering prior to down-stream analyses. Predefined subgroups and supervised clustering studies might give distorted results if they are based on pools of mixed tumour histopathology subgroups. In conclusion, we have identified *ERBB3* as a marker of a GNB/GN-like expression profile, and we suggest a 7-gene expression signature as a complement to histopathological assessment of neuroblastic tumours. Further studies of ErbB3 and other members of the ErbB family and their role in neuroblastic differentiation and pathogenesis are warranted.

Methods

Pre-processing microarray data

Data from five published neuroblastoma expression microarray studies run on three different Affymetrix platforms (HU133A, HGU95Av, and HU133plus2) were used in this study (Table 1). Raw data files were obtained from Array Express (www.ebi.ac.uk/microarray-as/ae/) and Gene Expression Omnibus (www.ncbi.nlm.nih.gov/geo/), or directly from collaborators. Expression data files were normalized by gcRMA using Bioconductor (library BioC 2.4) in R 2.9.2 [52] in four separate groups; 1) the De Preter [53] data set run on the HGU133A Affymetrix platform (17 samples, preamplified), 2) the McArdle [54] and the Wilzén [55] data sets run on the HGU133A Affymetrix platform (30 samples, not pre-amplified), 3) the Wang [56] data set run on the HGU95Av2 platform (102 samples, not pre-amplified), and 4) the Versteeg [57] data set run on the HU133plus2 platform (110 samples). For each probe-set, the maximum expression values over all samples were determined, and

probe-sets which showed very low or no detectable expression levels were filtered out (log2 expression <5). Next, the mean log2 expression level for each Gene symbol was calculated to generate “mean-per-gene” data files: 7439 genes in data set 1, 8106 genes in data set 2, 7542 genes in data set 3, and 15614 genes in data set 4.

Differential expression analysis

NB samples from the DePreter and McArdle/Wilzén data sets were divided into four r-subgroups by a 6-gene signature (further referred to as the “6-GeneSig”) according to Abel et al., 2011 [12] (Additional file 1). From these two data sets, 14 (preamplified, De Preter) and 23 (non-preamplified, McArdle/Wilzén) cases respectively were successfully assigned into one of the four r-groups (Table 1). Differential gene expression analysis was performed by a two group unpaired Significance Analysis of Microarray (SAM) test (*i.e.* six comparisons) [58]. Gene lists comprising the 1000 most significantly differentially expressed genes (sorted after the d-statistic) with a fold change above 2 were exported from each comparison, from each direction (up or down), and from each data set, separately (resulting in 12 SAM gene lists per data set). Next, SAM gene lists from the two different data sets were compared, and 12 intersection gene lists (SAM_{intersect}) were created. To minimize the variance, a combined fold change (FC_{comb}) for each gene in the SAM_{intersect} gene list was calculated as follows:

$$FC_{\text{comb}} = FC \frac{V_2}{1} FC \frac{V_1}{2}$$

where FC_i is the fold change in data set *i* and

$$V_i = \frac{SE_i^2}{SE_1^2 + SE_2^2}$$

where SE_i is the standard error of the mean log2 expression values in data set *i*.

A combined p-value (P_{comb}) for each gene in the SAM_{intersect} gene list was calculated as follows:

$$P_{\text{comb}} = \Phi \left(\sqrt{\frac{N_1}{N_1 + N_2}} \Phi^{-1}(P_1) + \sqrt{\frac{N_1}{N_1 + N_2}} \Phi^{-1}(P_2) \right)$$

where N_i is the total number of samples of the two groups compared by the

d-statistic in SAM, and P_i the corresponding p-value for dataset *i*. Φ is the cumulative distribution function of the standard normal distribution and Φ⁻¹ is its inverse function.

Based on an approximation of 8000 multiple tests (*i.e.* 8000 genes), a nominal p-value <6.25E-06 was found to correspond to an adjusted p-value <0.05 (according to Bonferroni correction) and was subsequently used as a cut-off for significance in SAM.

Gene network modelling

A large gene regulatory network was constructed from an independent data set (Wang) of 102 expression profiles [56]. Mutual information values were estimated with the ARACNE (Algorithm for the Reconstruction of Accurate Cellular Networks) algorithm using a p-value cut-off of 1E-7 [26]. The data processing inequality (DPI) was applied with a tolerance of 0.15. Gene networks of seven selected genes were extracted from the global network together with their immediate gene neighbours. The gene networks of nearest neighbours were visualized in Cytoscape 2.8.2.

Gene ontology (GO) and Gene Set enrichment analysis (GSEA)

Ranked SAM gene lists (by d-statistic) from the separate data sets were investigated for Gene Ontology terms using BiNGO 2.4 (Biological Network Gene Ontology, www.psb.ugent.be/cbd/papers/BiNGO/). The Gene Set Enrichment Analysis (GSEA, www.broad.mit.edu/gsea/) software was used to investigate whether a gene network was significantly overrepresented in the different r-subgroups. The enrichment tests were performed using seven ARACNE-constructed gene networks ALK (n = 12 genes), BIRC5 (n = 45 genes), CCND1 (n = 22 genes), ERBB3 (n = 38 genes), MYCN (n = 40 genes), NTRK1 (n = 62 genes), and PHOX2B (n = 67 genes), as well as 4850 MSigDB-curated gene sets (c2, www.broadinstitute.org/gsea/msigdb/index.jsp, Additional file 6). The GSEA according to Subramanian *et al.* [59], was run on the “mean-per-gene” data files using the following settings: number of permutations = 1000, permutation type = gene-set, chip platform = GENE_SYMBOL.chip, enrichment statistic = weighted, metric for ranking genes = Signal2Noise, gene list sorting mode = real, gene list ordering mode = descending, max gene set size = 500 (the default), min gene set size = 10 (the default is 15). In addition, the r3 versus r1 comparisons in data sets 1–3 were investigated according to the gene list sorting mode = abs.

Human tissue samples used for protein expression validation

Tumours histopathologically classified as GN and NB (data set 5, Table 1) were used for immunohistochemistry (4 NB and 4 GN), and immunoblot analysis (4 NB and 5 GN). Tissue from patients was obtained during surgery and stored in -80°C. Ethical approval was obtained from the Karolinska University Hospital Research Ethics Committee (Approval no. 2009/1369-31/1 and 03-736). Informed consent for using tumor samples in scientific research was provided by parents/guardians. In accordance with the approval from the Ethics Committee the informed consent was either written or verbal. When verbal or written assent was not obtained the decision was documented in the medical record.

Immunohistochemistry

Formalin-fixed and paraffin-embedded (FFPE) tissue slides were deparaffinized in xylol and rehydrated in graded alcohols. For antigen retrieval, slides were boiled in a sodium citrate buffer (pH 6.0) for 10 min, in a microwave oven. After blocking in 1% bovine serum albumin (BSA) for 20 min, the tissue sections were incubated with primary antibody overnight, Sox10 ([N-20], Santa Cruz Biotechnology) and ErbB-3 ([RTJ2], Abcam) respectively, diluted 1:50 in 1% PBSA. Thereafter slides were rinsed in PBS and endogenous peroxidases were blocked in 0.3% H₂O₂ for 10 min. As a secondary antibody, anti-mouse-horseradish peroxidase (HRP) and anti-goat-horseradish peroxidase were used (Invitrogen, Paisley, UK). All slides were counterstained with haematoxylin. To control for non-specific binding, antibody specific blocking peptides and isotype-matched controls were used. For colocalization studies of Erb3 and Sox10, tumor tissue sections were simultaneously stained with primary antibodies and for fluorescence visualization, anti-goat Alexa Fluor 594 and anti-mouse Alexa Fluor 488 were used, respectively.

Immunoblot analysis

Tumours were homogenized in RIPA buffer (20 mM Tris-HCl, pH 7.5, 150 mM NaCl, 1 mM Na₂EDTA, 1 mM EGTA, 1% NP-40, 1% sodium deoxycholate, 2.5 mM sodium pyrophosphate, 1 mM beta-glycerophosphate, 1 mM Na₃VO₄, 1 ug/ml leupeptin) with protease inhibitor cocktail (Roche), 42 mM DTT and 1 mM PMSF. The total protein concentration was determined using A280 absorbance readings and 100 ug of total protein was diluted in NuPAGE® LDS sample buffer (Invitrogen) with 50 mM DTT and denatured for 10 min at 70°C. The samples were then loaded with a prestained Page Ruler protein ladder (Thermo-Scientific) on a 4-12% NuPAGE® Bis-Tris polyacrylamide gel (Invitrogen) and separated using MOPS buffer at 200V for 50 min. The proteins were transferred to PVDF membranes using NuPAGE® transfer buffer (Invitrogen) and 10% methanol. Following Ponceau staining to ensure equal loading, membranes were washed with TBS-T (Tris-buffered saline containing 0.1% Tween 20) and blocked with blocking buffer (5% milk/TBS-T) for 1 h. The primary antibodies were added to the membranes and incubated overnight at 4°C. The following day, membranes were washed with TBS-T and incubated with secondary antibodies. Following final TBS-T washes, protein detection was achieved with Pierce Super Signal® West Pico or Femto Chemiluminescent Substrate (Thermo-Scientific). The primary antibodies used were anti-ErbB3 [RTJ2] (Abcam, 1:200) and anti-Gapdh (Abcam, #ab8245, 1:10000). The secondary antibodies used were anti-mouse IgG HRP linked antibodies (Cell Signaling, #7076, 1:5000), anti-rabbit IgG

HRP linked antibodies (Cell Signaling, #7074, 1:5000). All antibodies were diluted in blocking buffer.

Statistical analyses

The expression relationship of *ERBB3* to the discriminative 6-GeneSig (*ALK*, *BIRC5*, *CCND1*, *MYCN*, *NTRK1*, and *PHOX2B*) and the ErbB family members *EGFR*, *ERBB2*, and *ERBB4* were investigated by a Pearson correlation test. The statistical significance of expression levels of *ERBB* genes (i.e. *EGFR*, *ERBB2*, *ERBB3*, and *ERBB4*) were investigated by Welch t-test. Inter-rater reliability of group assignments was tested by the Kappa statistic on crosstabs in SPSS (version 20.0).

Additional files

Additional file 1: The 6-GeneSig subgroup classification rules. Rules based on standard deviations (SD) of expression values for all samples in each data set. In order for samples to be successfully assigned into one of four r-groups, 5 out of 6 expression rules must be met. Shaded cells indicate rules with no exception for classification into that specific subgroup.

Additional file 2: SAM results. The table presents the 1000 most significant genes in each direction from the SAM analyses of four data sets: 1 (DePreter), 2 (McArdleWilzén), 3 (Wang) and 4 (Versteeg). In addition, the $\text{SAM}_{\text{intersect}}$ gene lists are also presented (named DePreterMcArdleWilzén). Comparisons are named '12', '13', '14', '23' etc. corresponding to r2 versus r1, r3 versus r1, r4 versus r1, r3 versus r2, respectively. Directions of differential expressions are referred to as "up" and "down".

Additional file 3: GO results. The Biological Networks Gene Ontology tool (BINGO) in Cytoscape was utilized to map the predominant functional themes of the SAM gene lists. The 10 most significant Gene Ontology (GO) from terms in each SAM comparison are presented. Gene lists are divided into three data sets; data set 1 & 2 (DePreterMcArdleWilzén), data set 3 (Wang), data set 4 (Versteeg), and into two differential expression directions; "up" or "down". GO-ID: Gene Ontology identification number, p-val: p-value, corr p-val: corrected p-value, Description: Description of the gene ontology theme. The "DePreterMcArdleWilzén_12_down" list was too short (22 genes) to enable the GO term search.

Additional file 4: Correlations of ERBB3 to the 6-GeneSig other ERBB family members. Left panel: Pearson Correlations of *ERBB3* to the 6-gene signature (6-GeneSig) in four data sets separately (1 = De Preter, 2 = McArdle/Wilzén, 3 = Wang, 4 = Versteeg). Right panel: Pearson Correlations between the four *ERBB*-genes in four data sets separately. Positive correlations are marked in grey, and negative correlations are marked in white. Significance (2-tailed) is marked as follows: *Significant at the 0.05 level; **Significant at the 0.01 level; ***Significant at the 0.001 level. N = number of cases.

Additional file 5: TS candidate genes. Tumour suppressor genes were found by the PubMed search term "Neuroblastoma AND tumour suppressor", and from previous mining of literature lists according to Vermeulen et al., Lancet Oncol. 2009 July; 10(7): 663-671 (59 gene set) and Thorell et al., BMC Med Genomics 2009 Aug 17; 2:53. Present in $\text{SAM}_{\text{intersect}}$: genes found in the intersect SAM lists of data sets 1 & 2. y = yes; n = no.

Additional file 6: Gene networks used for GSEA analysis. The table presents the gene network members of all c2 curate gene sets (4850 in total) from MSigDB (www.broadinstitute.org/gsea/msigdb), and seven ARACNE gene networks used in the GSEA analyses.

Additional file 7: GSEA results. Results of Gene set enrichment analysis (GSEA) from each comparison and each data set are presented in each sheet. Data sets 1–3 (DePreter, McArdle/Wilzén, and Wang) comparisons

are according to r-subgroups (r1-r4), and data set 4 (Versteeg) comparisons are according to histopathology groups; Ganglioneuroma (GN), Ganglioneuroblastoma (GNB), and Neuroblastoma (NB). Enrichments were run with 1000 permutations, permutation type = gene set, and gene list sorting mode = real (scoring both extremes) in descending order. Results per data set and comparison in each sheet are presented as follows: NAME = name of the gene set, SIZE = Size of the gene set, ES = enrichment score, NES = Normalized enrichment score, NOM p-val = Nominal p-value, FDR q-val = False Discovery Rate, FWER p-val = Familywise-error rate, RANK AT MAX = The position in the ranked list at which the maximum enrichment score occurred, LEADING EDGE = Displays the three statistics used to define the leading edge subset. In addition, the r3 versus r1 comparisons in data sets 1–3 were investigated and presented as gene list sorting mode = abs.

Additional file 8: Analyses of the NTRK1 and MYCN gene networks.

Networks for MYCN (n = 40) and NTRK1 (n = 62) were created from the Wang data set using the ARACNE software (see text for details). Differentially expressed genes of r-groups are marked by coloured nodes; red = up-regulated, green = down-regulated. Left panel: Data sets 1 and 2 (DePreter and McArdle/Wilzén) presenting the r3 vs. r1 comparison for the MYCN- (upper) and NTRK1- networks (lower). Only genes that were common in both data set 1 and 2 with fold change > 2 were included (i.e. $\text{SAM}_{\text{intersect}}$ gene lists). Middle panel: Data set 3 (Wang) presenting the r3 vs. r1 comparison for the MYCN- (upper) and NTRK1- networks (lower). Genes included were those present in SAM gene list representing the 1000 most differentially expressed with fold change > 2 (ranked after significance). Right panel: Gene set enrichment analysis (GSEA) plots of the MYCN and NTRK1 networks are according to gene list sorting mode = real, sorted in descending order. NES = Normalized enrichment score, NOM p-val. = Nominal p-value, according to the GSEA results (see Additional file 7). *The NOM p-val. for the MYCN-network is presented according to gene list sorting mode = abs (see Additional file 7).

Additional file 9: The 7-GeneSig classification rules. Rules based on standard deviations (SD) of expression values for all samples in each data set. In order to classify samples into one of the five subgroups, 5 out of 6 expression rules must be met. Shaded cells indicate rules with no exception for classification into that specific subgroup.

Competing interests

The authors declare that no competing interests exist.

Authors' contributions

FA formulated the study design, and performed the microarray data pre-processing. AW and FA accomplished the analysis of SAM gene lists, GSEA, GO, and heat maps. AW and FA drafted the manuscript. CK performed the immunoblot analyses, and revised the manuscript. BS performed the immunohistochemistry analyses, and revised the manuscript. EK performed SAM analysis, and revised the manuscript. DD performed network modelling, and revised the manuscript. IØ performed the histopathology assessment of the Versteeg110 data set, and revised the manuscripts. KD, RS, JM, PK, and RV provided histopathology data as well as clinical data in terms of status of prognostic marker and survival of patients, and revised the manuscript. SN supervised the statistical analysis and interpretations of results, and revised the manuscript. All authors read and approved the final manuscript.

Acknowledgements

This work was supported by grants from the Swedish Medical Council and the Swedish Children's Cancer Foundation. RLS was supported by grants from Science Foundation Ireland (07/IN.1/B1776), Children's Medical and Research Foundation, and the U.S. National Institutes of Health (5R01CA127496). BS was supported by grants from Norwegian Cancer Society.

Author details

¹Department of Clinical Genetics, Institution of Biomedicine, Box 413, S- 405 30, Gothenburg University, Gothenburg, Sweden. ²Childhood Cancer Research Unit, Karolinska Institute, Astrid Lindgren Children's Hospital, Q6:05, S-171 76, Stockholm, Sweden. ³Department of Medical Biology, University of Tromsø, Tromsø, Norway. ⁴Department of Mathematical Statistics, Chalmers University of Technology, Gothenburg, Sweden. ⁵Department of Pediatric

Oncology, Clinical Sciences, Lund University, Lund, Sweden. ⁶Center for Medical Genetics, Ghent University Hospital, Ghent, Belgium. ⁷Department of Cancer Genetics, Royal College of Surgeons in Ireland and Children's Research Centre, Our Lady's Children's Hospital, Dublin, Ireland. ⁸Children's Hospital of Philadelphia, Division of Oncology, The University of Pennsylvania, Philadelphia, PA, USA. ⁹Department of Oncogenomics, Academic Medical Center, Meibergdreef 9, 1105AZ, Amsterdam, The Netherlands.

Received: 14 February 2013 Accepted: 25 June 2013

Published: 8 July 2013

References

- Shimada H, Ambros IM, Dehner LP, Hata J, Joshi VV, Roald B: Terminology and morphologic criteria of neuroblastic tumors: recommendations by the international Neuroblastoma pathology committee. *Cancer* 1999, **86**:349–363.
- Brodeur GM, Pritchard J, Berthold F, Carlsen NL, Castel V, Castelberry RP, De Bernardi B, Evans AE, Favrot M, Hedborg F, et al: Revisions of the international criteria for Neuroblastoma diagnosis, staging, and response to treatment. *J Clin Oncol* 1993, **11**:1466–1477.
- Monclair T, Brodeur GM, Ambros PF, Brisse HJ, Ceccchetto G, Holmes K, Kaneko M, London WB, Matthay KK, Nuchtern JG, et al: The international Neuroblastoma risk group (INRG) staging system: an INRG task force report. *J Clin Oncol* 2009, **27**:298–303.
- Breslow N, McCann B: Statistical estimation of prognosis for children with Neuroblastoma. *Cancer Res* 1971, **31**:2098–2103.
- Shimada H, Ambros IM, Dehner LP, Hata J, Joshi VV, Roald B, Stram DO, Gerbing RB, Lukens JN, Matthay KK, Castleberry RP: The international Neuroblastoma pathology classification (the Shimada system). *Cancer* 1999, **86**:364–372.
- Brodeur GM, Seeger RC, Schwab M, Varmus HE, Bishop JM: Amplification of N-myc in untreated human Neuroblastoma correlates with advanced disease stage. *Science* 1984, **224**:1121–1124.
- Caren H, Kryh H, Nethander M, Sjoberg RM, Trager C, Nilsson S, Abrahamsson J, Kogner P, Martinsson T: High-risk Neuroblastoma tumors with 11q-deletion display a poor prognostic, chromosome instability phenotype with later onset. *Proc Natl Acad Sci USA* 2010, **107**:4323–4328.
- Look AT, Hayes FA, Shuster JJ, Douglass EC, Castleberry RP, Bowman LC, Smith EL, Brodeur GM: Clinical relevance of tumor cell ploidy and N-myc gene amplification in childhood Neuroblastoma: a pediatric oncology group study. *J Clin Oncol* 1991, **9**:581–591.
- Cohn SL, Pearson AD, London WB, Monclair T, Ambros PF, Brodeur GM, Faldum A, Hero B, Ichihara T, Machin D, et al: The international Neuroblastoma risk group (INRG) classification system: an INRG task force report. *J Clin Oncol* 2009, **27**:289–297.
- Brodeur GM: Neuroblastoma: biological insights into a clinical enigma. *Nat Rev Cancer* 2003, **3**:203–216.
- Michels E, Vandesompele J, De Preter K, Hoebeeck J, Vermeulen J, Schramm A, Molenaar JJ, Merten B, Marques B, Stallings RL, et al: ArrayCGH-based classification of Neuroblastoma into genomic subgroups. *Genes Chromosomes Cancer* 2007, **46**:1098–1108.
- Abel F, Dalevi D, Nethander M, Jornsten R, De Preter K, Vermeulen J, Stallings R, Kogner P, Maris J, Nilsson S: A 6-gene signature identifies four molecular subgroups of Neuroblastoma. *Cancer cell international* 2011, **11**:9.
- Buckley PG, Alcock L, Bryan K, Bray I, Schulte JH, Schramm A, Eggert A, Mestdagh P, De Preter K, Vandesompele J, et al: Chromosomal and microRNA expression patterns reveal biologically distinct subgroups of 11q- Neuroblastoma. *Clin Cancer Res* 2010, **16**:2971–2978.
- De Preter K, De Brouwer S, Van Maerken T, Pattyn F, Schramm A, Eggert A, Vandesompele J, Speleman F: Meta-mining of Neuroblastoma and neuroblast gene expression profiles reveals candidate therapeutic compounds. *Clin Cancer Res* 2009, **15**:3690–3696.
- De Preter K, Mestdagh P, Vermeulen J, Zeka F, Naranjo A, Bray I, Castel V, Chen C, Drozynska E, Eggert A, et al: miRNA expression profiling enables risk stratification in archived and fresh Neuroblastoma tumor samples. *Clin Cancer Res* 2011, **17**:7684–7692.
- De Preter K, Vermeulen J, Brors B, Delattre O, Eggert A, Fischer M, Janoueix-Lerosey I, Lavarino C, Maris JM, Mora J, et al: Accurate outcome prediction in Neuroblastoma across independent data sets using a multigene signature. *Clin Cancer Res* 2010, **16**:1532–1541.
- Obertuer A, Hero B, Berthold F, Juraeva D, Faldum A, Kahler Y, Asgharzadeh S, Seeger R, Scaruffi P, Tonini GP, et al: Prognostic impact of gene expression-based classification for Neuroblastoma. *J Clin Oncol* 2010, **28**:3506–3515.
- Schulte JH, Schow B, Mestdagh P, Kaderali L, Kalaghati P, Schlierf S, Vermeulen J, Brockmeyer B, Pajtler K, Thor T, et al: Accurate prediction of Neuroblastoma outcome based on miRNA expression profiles. *Int J Cancer* 2010, **127**:2374–2385.
- Vermeulen J, De Preter K, Laureys G, Speleman F, Vandesompele J: 59-gene prognostic signature sub-stratifies high-risk Neuroblastoma patients. *Lancet Oncol* 2009, **10**:1030.
- Molenaar JJ, Koster J, Ebus ME, van Sluis P, Westerhout EM, de Preter K, Gisselsson D, Ora I, Speleman F, Caron HN, Versteeg R: Copy number defects of G1-cell cycle genes in Neuroblastoma are frequent and correlate with high expression of E2F target genes and a poor prognosis. *Genes Chromosomes Cancer* 2012, **51**:10–19.
- Valentijn LJ, Koster J, Haneweld F, Aissa RA, van Sluis P, Broekmans ME, Molenaar JJ, van Nes J, Versteeg R: Functional MYCN signature predicts outcome of Neuroblastoma irrespective of MYCN amplification. *Proc Natl Acad Sci USA* 2012, **109**:19190–19195.
- Caren H, Abel F, Kogner P, Martinsson T: High incidence of DNA mutations and gene amplifications of the ALK gene in advanced sporadic Neuroblastoma tumours. *Biochem J* 2008, **416**:153–159.
- De Brouwer S, De Preter K, Kumps C, Zabrocki P, Porcu M, Westerhout EM, Lakeman A, Vandesompele J, Hoebeeck J, Van Maerken T, et al: Meta-analysis of Neuroblastoma reveals a skewed ALK mutation spectrum in tumors with MYCN amplification. *Clin Cancer Res* 2010, **16**:4353–4362.
- Passoni L, Longo L, Collini P, Coluccia AM, Bozzi F, Podda M, Gregorio A, Gambini C, Garaventa A, Pistoia V, et al: Mutation-independent anaplastic lymphoma kinase overexpression in poor prognosis Neuroblastoma patients. *Cancer Res* 2009, **69**:7338–7346.
- Sithanandam G, Anderson LM: The ERBB3 receptor in cancer and cancer gene therapy. *Cancer Gene Ther* 2008, **15**:413–448.
- Margolin AA, Wang K, Lim WK, Kustagi M, Nemenman I, Califano A: Reverse engineering cellular networks. *Nat Protoc* 2006, **1**:662–671.
- Allen JD, Xie Y, Chen M, Girard L, Xiao G: Comparing statistical methods for constructing large scale gene networks. *PLoS One* 2012, **7**:e29348.
- Lamers F, van der Ploeg I, Schild L, Ebus ME, Koster J, Hansen BR, Koch T, Versteeg R, Caron HN, Molenaar JJ: Knockdown of surviving (BIRC5) causes apoptosis in Neuroblastoma via mitotic catastrophe. *Endocr-Related Cancer* 2011, **18**:657–668.
- Katoh M, Igarashi M, Fukuda H, Nakagama H, Katoh M: Cancer genetics and genomics of human FOX family genes. *Cancer Lett* 2013, **328**:198–206.
- Eckerle I, Muth D, Batzler J, Henrich KO, Lutz W, Fischer M, Witt O, Schwab M, Westermann F: Regulation of BIRC5 and its isoform BIRC5-2B in Neuroblastoma. *Cancer Lett* 2009, **285**:99–107.
- Otto T, Horn S, Brockmann M, Eilers U, Schuttrumpf L, Popov N, Kenney AM, Schulte JH, Beijersbergen R, Christiansen H, et al: Stabilization of N-Myc is a critical function of Aurora A in human Neuroblastoma. *Cancer cell* 2009, **15**:67–78.
- Munirajan AK, Ando K, Mukai A, Takahashi M, Suenaga Y, Ohira M, Koda T, Hirota T, Ozaki T, Nakagawara A: KIF1Bbeta functions as a haploinsufficient tumor suppressor gene mapped to chromosome 1p36.2 by inducing apoptotic cell death. *J Biol Chem* 2008, **283**:24426–24434.
- Schlioso S, Kenchappa RS, Vredeveld LC, George RE, Stewart R, Greulich H, Shahriari K, Nguyen NV, Pigny P, Daha PL, et al: The kinesin KIF1Bbeta acts downstream from EgfN3 to induce apoptosis and is a potential 1p36 tumor suppressor. *Genes Dev* 2008, **22**:884–893.
- Fujita T, Igarashi J, Okawa ER, Gotoh T, Manne J, Kolla V, Kim J, Zhao H, Pawel BR, London WB, et al: CHD5, a tumor suppressor gene deleted from 1p36.31 in Neuroblastoma. *J Natl Cancer Inst* 2008, **100**:940–949.
- Brodeur GM, Fong CT, Morita M, Griffith R, Hayes FA, Seeger RC: Molecular analysis and clinical significance of N-myc amplification and chromosome 1p monosomy in human Neuroblastoma. *Prog Clin Biol Res* 1988, **271**:3–15.
- Molenaar JJ, Koster J, Zwijnenburg DA, van Sluis P, Valentijn LJ, van der Ploeg I, Hamdi M, van Nes J, Westerman BA, van Arkel J, et al: Sequencing of Neuroblastoma identifies chromothripsis and defects in neuritogenesis genes. *Nature* 2012, **483**:589–593.

37. Mocellin S, Zavagno G, Nitti D: The prognostic value of serum S100B in patients with cutaneous melanoma: a meta-analysis. *Int J Cancer* 2008, **123**:2370–2376.

38. Levy P, Vidaud D, Leroy K, Laurendeau I, Wechsler J, Bolasco G, Parfait B, Wolkenstein P, Vidaud M, Bieche I: Molecular profiling of malignant peripheral nerve sheath tumors associated with neurofibromatosis type 1, based on large-scale real-time RT-PCR. *Mol Cancer* 2004, **3**:20.

39. Satge D, Sasco AJ, Carlsen NL, Stiller CA, Rubie H, Hero B, de Bernardi B, de Kraker J, Coze C, Kognor P, et al: A lack of Neuroblastoma in Down syndrome: a study from 11 European countries. *Cancer Res* 1998, **58**:448–452.

40. Britsch S, Goerich DE, Riethmacher D, Peirano RI, Rossner M, Nave KA, Birchmeier C, Wegner M: The transcription factor Sox10 is a key regulator of peripheral glial development. *Genes Dev* 2001, **15**:66–78.

41. Buac K, Watkins-Chow DE, Loftus SK, Larson DM, Incao A, Gibney G, Pavan WJ: A Sox10 expression screen identifies an amino acid essential for Erbb3 function. *PLoS Genet* 2008, **4**:e1000177.

42. Addo-Yobo SO, Straessle J, Anwar A, Donson AM, Kleinschmidt-Demasters BK, Foreman NK: Paired overexpression of ErbB3 and Sox10 in pilocytic astrocytoma. *J Neuropathol Exp Neurol* 2006, **65**:769–775.

43. Karamchandani JR, Nielsen TO, van de Rijn M, West RB: Sox10 and S100 in the diagnosis of soft-tissue neoplasms. *Appl Immunohistochem Mol Morphol* 2012, **20**:445–450.

44. Acosta S, Lavarino C, Paris R, Garcia I, de Torres C, Rodriguez E, Beleta H, Mora J: Comprehensive characterization of Neuroblastoma cell line subtypes reveals bilineage potential similar to neural crest stem cells. *BMC Dev Biol* 2009, **9**:12.

45. Holbro T, Beerli RR, Maurer F, Koziczk M, Barbas CF 3rd, Hynes NE: The ErbB2/ErbB3 heterodimers functions as an oncogenic unit: ErbB2 requires ErbB3 to drive breast tumor cell proliferation. *Proc Natl Acad Sci USA* 2003, **100**:8933–8938.

46. Ho R, Minturn JE, Hishiki T, Zhao H, Wang Q, Cnaan A, Maris J, Evans AE, Brodeur GM: Proliferation of human neuroblastomas mediated by the epidermal growth factor receptor. *Cancer Res* 2005, **65**:9868–9875.

47. Hua Y, Gorshkov K, Yang Y, Wang W, Zhang N, Hughes DP: Slow down to stay alive: HER4 protects against cellular stress and confers chemo resistance in Neuroblastoma. *Cancer* 2012, **118**:5140–5154.

48. Izycka-Swieszewska E, Wozniak A, Drozynska E, Kot J, Grajkowska W, Klepacka T, Perek D, Koltan S, Bien E, Limon J: Expression and significance of HER family receptors in neuroblastic tumors. *Clin Exp Metastasis* 2011, **28**:271–282.

49. Peuchmaur M, d'Amore ES, Joshi W, Hata J, Roald B, Dehner LP, Gerbing RB, Stram DO, Lukens JN, Matthay KK, Shimada H: Revision of the international Neuroblastoma pathology classification: confirmation of favorable and unfavorable prognostic subsets in ganglioneuroblastoma, nodular. *Cancer* 2003, **98**:2274–2281.

50. Van Ho AT, Hayashi S, Brohl D, Aurade F, Rattenbach R, Relaix F: Neural crest cell lineage restricts skeletal muscle progenitor cell differentiation through Neuregulin1-ErbB3 signaling. *Dev Cell* 2011, **21**:273–287.

51. Izycka-Swieszewska E, Wozniak A, Kot J, Grajkowska W, Balcerska A, Perek D, Dembowska-Baginska B, Klepacka T, Drozynska E: Prognostic significance of HER2 expression in neuroblastic tumors. *Mod Pathol* 2010, **23**:1261–1268.

52. Gentleman RC, Carey VJ, Bates DM, Bolstad B, Dettling M, Dudoit S, Ellis B, Gautier L, Ge Y, Gentry J, et al: Bio conductor: open software development for computational biology and bioinformatics. *Genome Biol* 2004, **5**:R80.

53. De Preter K, Vandesompele J, Heimann P, Yigit N, Beckman S, Schramm A, Eggert A, Stallings RL, Benoit Y, Renard M, et al: Human fetal neuroblast and Neuroblastoma transcriptome analysis confirms neuroblast origin and highlights Neuroblastoma candidate genes. *Genome Biol* 2006, **7**:R84.

54. McArdle L, McDermott M, Purcell R, Grehan D, O'Meara A, Breathnach F, Catchpoole D, Culhane AC, Jeffery I, Gallagher WM, Stallings RL: Oligonucleotide microarray analysis of gene expression in Neuroblastoma displaying loss of chromosome 11q. *Carcinogenesis* 2004, **25**:1599–1609.

55. Wilzén A, Nilsson S, Sjöberg R, Martinsson T, Abel F: The Phox2 pathway is suppressed in high risk Neuroblastoma tumors, but does not involve mutations of the candidate tumor suppressor gene PHOX2A. 2008.

56. Wang Q, Diskin S, Rappaport E, Attiyeh E, Mosse Y, Shue D, Seiser E, Jagannathan J, Shusterman S, Bansal M, et al: Integrative genomics identifies distinct molecular classes of Neuroblastoma and shows that multiple genes are targeted by regional alterations in DNA copy number. *Cancer Res* 2006, **66**:6050–6062.

57. Revet I, Huizinga G, Chan A, Koster J, Volckmann R, van Sluis P, Ora I, Versteeg R, Geerts D: The MSX1 home box transcription factor is a downstream target of PHOX2B and activates the Delta-Notch pathway in Neuroblastoma. *Exp Cell Res* 2008, **314**:707–719.

58. Tusher VG, Tibshirani R, Chu G: Significance analysis of microarrays applied to the ionizing radiation response. *Proc Natl Acad Sci USA* 2001, **98**:5116–5121.

59. Subramanian A, Tamayo P, Mootha VK, Mukherjee S, Ebert BL, Gillette MA, Paulovich A, Pomeroy SL, Golub TR, Lander ES, Mesirov JP: Gene set enrichment analysis: a knowledge-based approach for interpreting genome-wide expression profiles. *Proc Natl Acad Sci USA* 2005, **102**:15545–15550.

doi:10.1186/1476-4598-12-70

Cite this article as: Wilzén et al.: ERBB3 is a marker of a ganglioneuroblastoma/ganglioneuroma-like expression profile in neuroblastic tumours. *Molecular Cancer* 2013 12:70.

Submit your next manuscript to BioMed Central and take full advantage of:

- Convenient online submission
- Thorough peer review
- No space constraints or color figure charges
- Immediate publication on acceptance
- Inclusion in PubMed, CAS, Scopus and Google Scholar
- Research which is freely available for redistribution

Submit your manuscript at
www.biomedcentral.com/submit

